Journal of Manufacturing Systems
Vol. 20/No. 1
2001

Optimal Fixture Design for Drilling Through Deformable Plate Workpieces Part I: Model Formulation

K.R. Wardak, U. Tasch, and **P.G. Charalambides,** Dept. of Mechanical Engineering, University of Maryland Baltimore County, Baltimore, Maryland, USA

Abstract

This is the first part of two manuscripts that address the development of scientifically based methodologies that use finite element methods and optimization algorithms to design optimal fixturing layouts for the drilling process. Part I focuses on the problem formulation and Part II discusses the results. The fixturing problem formulation is posed as a constrained optimization problem, in which the physical fixture constraints define the domain, and the desired fixturing characteristics are optimized in accordance with a selected objective function. The optimal fixturing model developed includes a material removal strategy that enables one to calculate the shape and dimensions of the machined hole surface. The boundary value problem associated with the optimal fixturing simulations is first formulated. Five different objective functions capable of describing various geometrical aspects of the machined hole have been developed and tested. These functions evaluate the square differences between the simulated and nominal radii and diameter values, minimize the maximum values of the latter quantities, and minimize the deviations of the drilled surface from a perfect cylinder.

Keywords: *Optimal, Fixture, Deformable, Workpiece, Drilling, Design, Objective Function, Finite Elements*

1. Introduction

Approximately 40% of rejected parts are due to dimensioning errors that are attributed to poor fixturing design.[1] Fixtures are used to accurately position and adequately constrain a workpiece in the machine-tool coordinate system. Adequate constraints of a deformable workpiece ensure that the dimensions and shape of the machined surfaces are within the required tolerances. Research efforts that address the development of scientifically based fixture design methodologies are reported in Refs. 2 through 10. Mathematical tools that are based on computer-aided design (CAD) and finite element (FE) analysis have been instrumental in advancing state-of-the-art fixture design methodologies.

This paper is structured as a two-part manuscript in which the model formulation is discussed in Part I and the results in Part II. (Part II follows in this issue.) Part I further develops the scientific tools that capture the shape and dimensional characteristics of the machined surfaces generated through drilling operations. These tools are based on FE analysis, optimization, and schemes that handle material removal strategies. In formulating the fixturing optimization problem, Part I presents five different objective functions that result in different fixture layouts. These layouts are tested and evaluated in Part II. A literature review that highlights the contributions of previous researchers follows.

Shirinzadeh[2] introduced reconfigurable fixture modules that are assembled by robotic manipulators and based on a CAD model of the workpiece. Automatically reconfigurable fixture designs are also addressed by earlier reports of Asada and By[3] and Chou et al.[4]; however, these concepts have been limited to laboratory applications. Automatic fixturing design[5] retains resting equilibrium and static stability of the workpiece. Resting equilibrium conditions are essential for stabilizing the workpiece when it is initially placed on the fixture locators, and static stability must be maintained when the clamping and machining forces are applied. A resting equilibrium is obtained when the wrench formed by the reacting locator-forces falls within the triangle formed by the three supporting locators; static stability is obtained if the matrix formed by the static equilibrium equations is fully ranked.

Brost and Goldberg[6] formulated optimal fixturing designs that minimize the reaction forces at the locators. In this formulation, the workpiece is modeled as a rigid body and the deformations induced by the clamping and machining forces are not considered. Zhang et al.[7] compared the optimal fixturing designs obtained through rigid body analysis to fixtures cal-

culated by elastically deformable workpiece models. Their findings demonstrate that the two formulations result in substantially different optimal fixturing layouts.

Lee and Haynes[8] and Menassa and DeVries[9] employed FE models to, respectively, obtain fixtures that minimize the work done by the clamping and machining forces and minimize the displacements of selected nodes of the FE mesh. Pong[10] introduced frictional contact elements to the FE models and incorporated formulations that minimize the displacements of selected FE nodes as well.

De Meter[11] applied optimization techniques to fixturing design based on contact region loading, where the workpiece is treated as a rigid body. Here, the selected objective function is the summation of the magnitudes of the loads in the contact regions. Melkote,[12] on the other hand, used genetic optimization algorithms to determine the layout of fixtures in which the deformation of the machined surface due to clamping and machining forces is minimized over the entire tool path.

Liao, Hu, and Stephenson[13] optimized fixture layouts by minimizing workpiece deflections due to clamping forces; nevertheless, the effects of machining forces are not accounted for. In this model, the deformations of the workpiece and locators are accounted for, and the interface between the locator and the workpiece is modeled as a surface contact pair. 3-2-1 fixturing scenarios are considered, and FEA is used to solve the deformation field. The deformations of selected nodes constitute the objective function. In addressing fixturing problems of deformable sheet metal that is neither prismatic nor solid, an N-2-1 fixture design has been proposed by Cai, Hu, and Yuan.[14] They report algorithms for finding the best N locating points such that total deformation of a sheet metal is minimized. These algorithms are based on the N-2-1 fixturing scenarios. Here, FEA models and nonlinear programming are utilized to obtain the optimal fixture layout.

Sayeed and De Meter[15] introduced a Mixed Integer Programming (MIP) model for determining the optimal locations of locator buttons and their opposing clamps for minimizing the effect of static workpiece deformations on machined feature geometric error. This model utilizes finite element analysis of the workpiece, yet its solution is size sensitive to the square of the number of machining response points considered. A technique that makes the MIP model size strictly proportional to the number of machining response points and alleviates this severe limitation is reported in Sayeed and De Meter.[16] Another fixture optimization algorithm was suggested by De Meter,[17] who presented Fast Support Layout Optimization (FSLO) models. FSLO determines support locations that minimize the maximum displacement-to-tolerance ratio of a set of workpiece features subject to machining loads. This work is highly relevant to the work presented in this manuscript.

The focus of the current research project is to develop scientific methods that capture the shape and geometry of machined surfaces generated through drilling operations and to design fixtures that maintain dimensional errors within allowable tolerances. Part I is organized as follows: the finite element formulation of the surface geometry generated through the drilling process is presented, and automatic mesh generation procedures are discussed. This is followed by a derivation of the optimal fixturing problem for which five different objective functions are suggested. Then, conclusions are reached.

2. Finite Element Modeling

In this study, the method of finite elements is employed for the purpose of calculating the workpiece deformations induced by the drilling loads. It is understood that the actual drilling process may be governed by nonlinear interactions between the penetrating drill and the deforming workpiece. For example, the removal of material during drilling alters the geometry and thus the structural stiffness of the workpiece, which in turn leads to higher deformations, both in the near-drill proximity as well as in remote regions of the workpiece. In addition to the local and global effects of material removal, nonlinear damage evolution in the near-drill proximity is also expected to augment the local deformation field, which determines the quality of the drilling process. This may include several types of damage such as microcracking in ceramics, delamination in composite laminates, plasticity in metals, fiber debonding and pull-out in fiber reinforced composites, and other potential forms of damage. To account for all of the above, a robust nonlinear finite element model needs to be developed. Such a nonlinear and computationally inten-

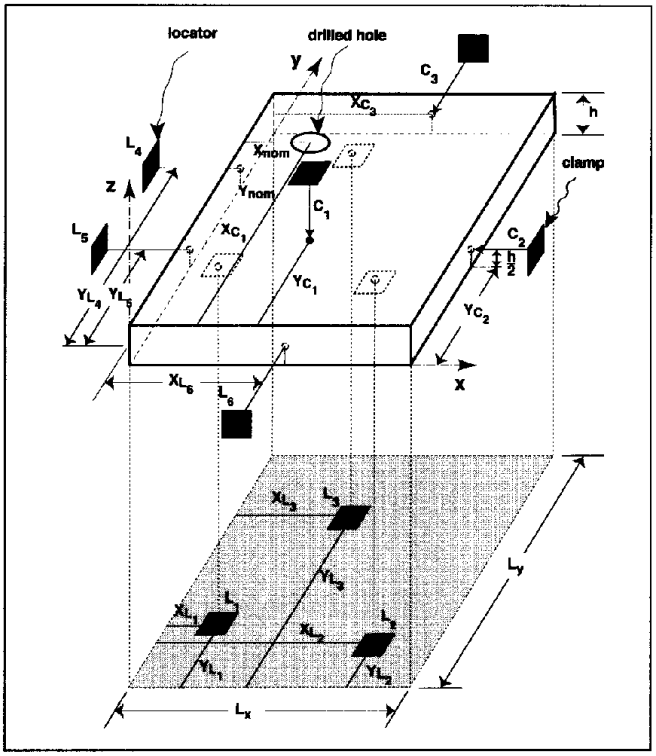

Figure 1
Fixturing Layout of a Prismatic Workpiece. L_1, L_2, and L_3 are the vertical locators; L_4, L_5, and L_6 are lateral locators; C_1 is a vertical clamp and C_2 and C_3 are lateral clamps.

sive model will then need to be embedded within an iterative optimization scheme. This optimization scheme is designed to assess the quality of the drilling process with built-in capabilities of identifying optimal restraining fixture configurations. While such a far-reaching modeling objective is now being considered, in this study we adopt a rather simplistic approach in simulating the drilling process using the method of finite elements. The boundary value problem and the assumptions used in the development of the finite element model in this study are presented next.

The study is conducted with the aid of the plate workpiece geometry shown in *Figure 1*. The plate has a length L_x, width L_y, and height h. The subscripts x, y, and z are used to indicate the plate alignment with respect to the global system of reference, the origin of which is located at the lower left corner of the plate. Vertical supports $L_1(X_{L_1}, Y_{L_1}, 0)$, $L_2(X_{L_2}, Y_{L_2}, 0)$, and $L_3(X_{L_3}, Y_{L_3}, 0)$ are placed at the bottom surface of the plate, and lateral restraints labeled as $L_4(0, Y_{L_4}, \frac{h}{2})$, $L_5(0, Y_{L_5}, \frac{h}{2})$, and $L_6(0, Y_{L_6}, \frac{h}{2})$ are introduced as needed to effectively restrain the in-plane rigid body motion of the workpiece. Clamps denot-

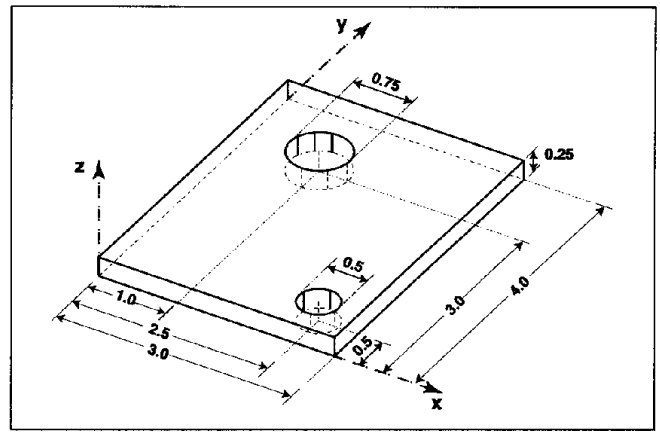

Figure 2
1/2 in. and 3/4 in. Holes are Drilled Through a 3x4x1/4 in. Plate. Centers are located at (2.5, 0.5) and (1.0, 3.0) (in.), respectively.

ed by $C_1(X_{C_1}, Y_{C_1}, h)$, $C_2(L_x, Y_{C_2}, \frac{h}{2})$, and $C_3(X_{C_3}, L_y, \frac{h}{2})$ are introduced to ensure total restraint. This application of the fixturing components is consistent with the 3-2-1 fixturing scheme utilized for prismatic workpieces (Refs. 2-10). Finally, a concentrated thrust force F_z and a line-distributed drilling torque M are imposed at the drilling site located at position (X_0, Y_0, Z_0).

As will be discussed later in this section, a general geometry model that is capable of simulating self-similar geometry, restraining, and loading configurations is first developed. However, the simulations conducted as part of this study are carried out for drilling various combinations of two holes through a plate dimensioned as shown in *Figure 2*.

For either the general or the specific problem considered in this study, the models are developed so that the optimization design variables are: the Cartesian coordinates of the three vertical locators (X_{L_i}, Y_{L_i}), i = 1–3, the Cartesian coordinates of the horizontal locators, (Y_{L_4}, Y_{L_5}, and X_{L_6}), the position of the vertical and horizontal clamps (X_{C_1}, Y_{C_1}, Y_{C_2}, and X_{C_3}), and the magnitude of the clamping forces ($F_{C_{Z_1}}$, $F_{C_{X_2}}$, and $F_{C_{Y_3}}$). This list of 16 design optimization parameters is denoted as $\bar{u}$. The parameters are the dependent variables of the objective functions defined in Section 4.

Geometry Discretization

A parametric mesh generator that is capable of discretizing the geometry shown in *Figure 1* has been developed. Here, 20-noded brick isoparametric elements are used. Geometry parameters such as plate length, width, height, hole location and diame-

ter, and hole depth and number of holes can be varied either internally through a user-specific algorithm or externally through a user-control input file. The mesh generator then establishes the spatial positioning of the nodes of critical 20-noded isoparametric super-elements, which are subdivided into the smaller finite elements based on further user input. Special care is given so that the final mesh exhibits nodal characteristics needed for the effective enforcement of the geometric and loading boundary conditions. Typical 3-D meshes generated with the aid of the generalized mesh generator for plates containing one, two, three, or four holes are shown in *Figures 3a-3d.*

These meshes contain anywhere between 648 (*Figure 3a*) and 936 (*Figure 3d*) 20-noded brick elements with about 11,000 to 16,000 degrees of freedom. Elastic solutions obtained using the above meshes and the sparse solver option of the ABAQUS[18] finite element software required approximately 1 to 2 minutes of cpu time on an SGI Challenge R10000 series machine. In most cases reported here, the optimal solutions required over 1000 iterations, within which a new elastic solution is generated.

Drilling Process Simulation

As discussed earlier in this work, the drilling process is a highly nonlinear phenomenon governed by material, geometric, and contact nonlinearities. To accurately simulate such a process, one needs to employ an incremental finite element scheme embedded in an iterative optimization algorithm. Thus, tens or possibly hundreds of thousands of finite element incremental solutions are required to be completed in conducting optimal drilling simulations. While such a task may be computationally feasible for future studies, in this work it was sought to derive useful insights on optimal fixturing by simulating drilling as a linear process.

More specifically, it is assumed that no damage of any form develops during drilling. It is assumed that the contact between the drill bit and the elastically deforming plate gives rise to constant drilling loads, which are modeled as a drilling concentrated thrust, F_z, and a line-distributed drilling torque, M.[19] Consequently, the material is removed in one step, greatly reducing the needed computations. As such, the drilling process is simulated by considering a preexisting terminal cylindrical hole in the plate of

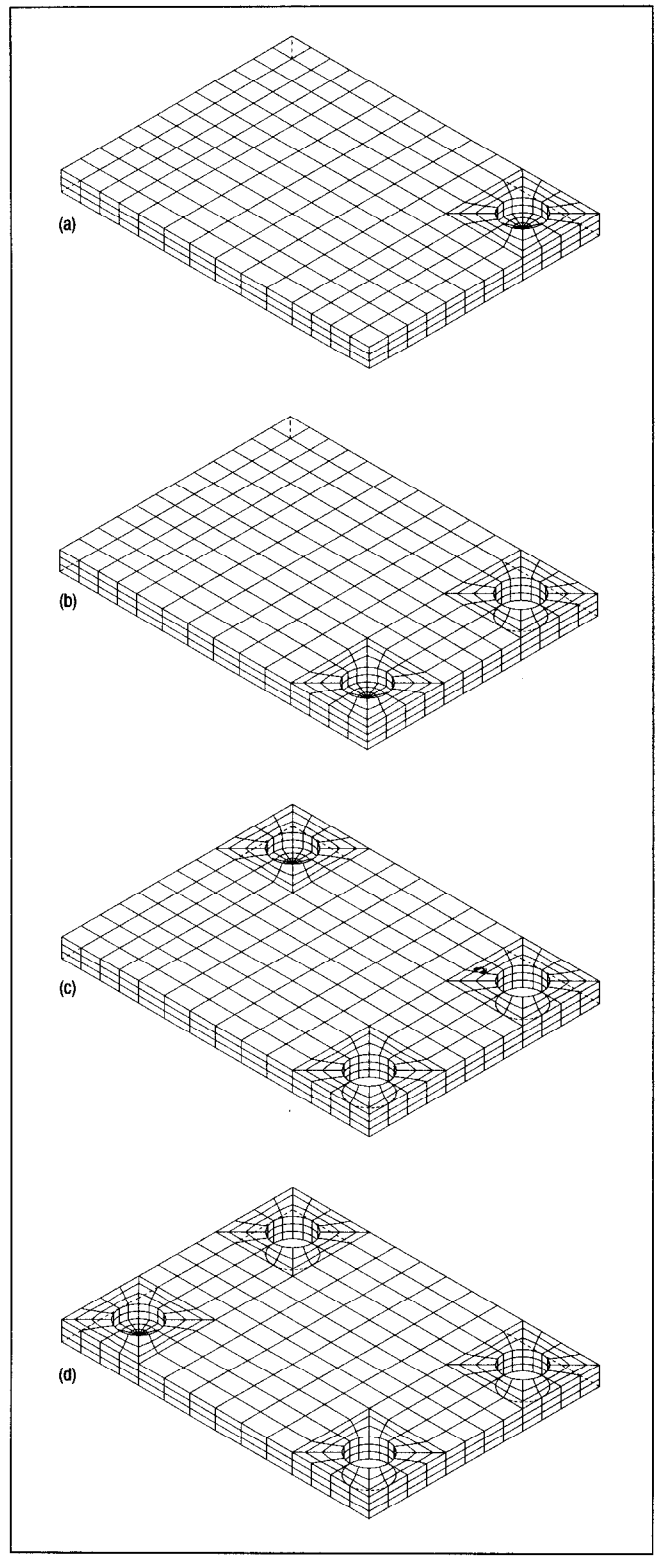

Figure 3
FE Meshes for a Single Hole (a), Two Holes (b), Three Holes (c), and Four Holes (d). The above undeformed meshes contain 648, 744, 840, and 936 20-noded isoparametric elements, respectively. Total number of degrees of freedom for (a), (b), (c), and (d) is 10,899, 12,582, 14,265, and 15,948, respectively.

diameter equal to that of the drill bit. The drilling thrust and moment developed at the leading front of the drilling process are thus introduced as applied loads acting on the bottom surface of the hole, as shown schematically in *Figure 4*. In the simulations reported here, a hole depth was selected to be equal to (0.9 *h*) throughout the study. This selection was based on solution convergence studies wherein the radial displacement component at the rim of the hole was monitored as a function of the hole depth. One may argue that modeling the drilling process using a preexisting hole reduces the overall stiffness of the workpiece, which introduces inaccuracies. It is important to state that in developing the current one-step drilling model, the above issue was considered and found to be irrelevant because at the end of the drilling process one encounters a weakened workpiece that is consistent with the current preexisting hole model.

The effects of the abovementioned drilling loads on an elastic workpiece constrained in a manner shown in *Figure 1* can be understood with the aid of *Figures 5a* and *5b*. In these figures, a top view of the entire workpiece as well as a view of a detailed region around the hole are shown. It is clear from the above deformed configurations that the elastic solution predicts physically inadmissible material interpenetration at the drill bit walls. To eliminate such physically inadmissible deformations, inverse mapping procedures are developed as needed to calculate and remove the interpenetrating material volume in the hole wall region, as shown schematically in *Figure 6*.

Once calculated, the interpenetrating material is removed as shown in *Figure 6b*, thus establishing frictionless contact between the plate at its deformed state and the rigid drill bit. Upon removal of the machining and clamping loads, the plate assumes an unloaded state at which the trimmed hole wall region recedes away from an initially cylindrical configuration to form a three-dimensionally complex conical hole (see *Figure 6c*). As will be discussed, the latter, three-dimensionally complex hole shape will be subjected to optimization with the aid of one of several objective functions that are also developed as part of this work. It is thus critically important to develop robust techniques capable of extracting from a 3-D finite element solution the hole shape obtained in the drilling process. The mathematical formulation of such a technique is presented next.

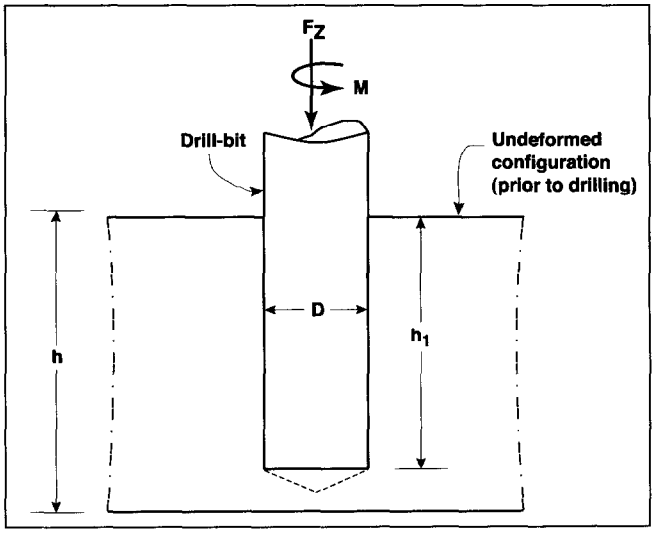

Figure 4
Detailed Schematic of Drilling Region. The applied thrust F_z and torque M are used to simulate the loads associated with the drilling process.

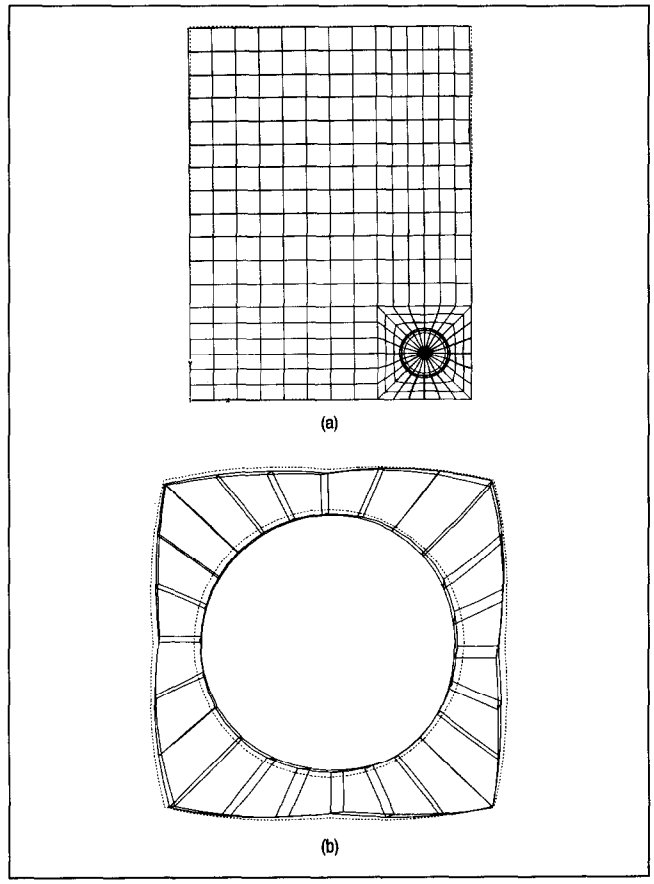

Figure 5
(a) Top View of a Deformed Finite Element Mesh obtained for a plate workpiece subjected to the F_z and M drilling loads and fixturing geometric conditions consistent with those shown in *Figure 1*.
(b) Closeup of Hole Boundary. Deformed mesh is depicted in solid lines and undeformed mesh in dashed lines.

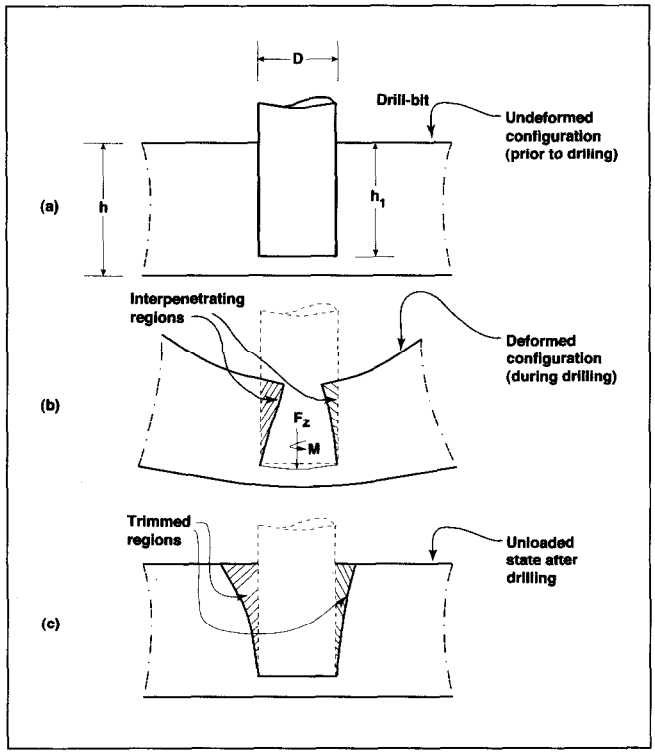

Figure 6
Simulation of Drilling Process. (a) A drill bit with diameter *D* placed in a preexisting hole of depth h_1. (b) Drilling loads of thrust F_z and torque *M* are applied and the workpiece is deformed. The material interpenetrating workpiece/drill bit region is removed. (c) Drilling loads are relaxed and the workpiece relaxes to its unloaded state.

3. Hole Shape Calculation Using Inverse Isoparametric Mapping

Consider a two-dimensional eight-noded isoparametric element that in its undeformed state is located at the boundary of the hole surface as shown in *Figure 7*. The coordinates (X_A,Y_A) of a point A in the interior of the element can be expressed as a weighted sum of the element nodal coordinates (X_i,Y_i), i = 1 – 8, as follows:

$$X_A = \sum_{i=1}^{8} N_i(\xi,\eta)X_{i_N}$$
$$Y_A = \sum_{i=1}^{8} N_i(\xi,\eta)Y_{i_N} \quad (1)$$

In Eq. (1), $N_i(\xi, \eta)$, i = 1 – 8, are the isoparametric nodal shape functions and ξ and η are the coordinates in the normalized isoparametric space. Through such an isoparametric mapping, the physical domain occupied by the above element is mapped to a normalized domain bounded by $-1 \le \xi \le +1$ and $-1 \le \eta \le +1$. Similarly, the displacement components u_A and v_A at the same point A are also expressed in terms of their nodal counterparts $(u_{i_N},v_{i_N}, i$ = 1 – 8) through a similar weighted summation:

$$u_A = \sum_{i=1}^{8} N_i(\xi,\eta)u_{i_N}$$
$$v_A = \sum_{i=1}^{8} N_i(\xi,\eta)v_{i_N} \quad (2)$$

Let point A after deformation assume a new position A' located at $(X_{A'},Y_{A'})$ on the admissible drilled surface, as shown in *Figure 7*. The position of the latter can be obtained from the original coordinates and the associated displacements at point A as follows:

$$X_{A'} = X_A + u_A = \sum_{i=1}^{8} N_i(\xi,\eta)\left(X_{i_N} + u_{i_N}\right)$$
$$Y_{A'} = Y_A + v_A \sum_{i=1}^{8} N_i(\xi,\eta)\left(Y_{i_N} + v_{i_N}\right) \quad (3)$$

Equation (3) can be used to extract the isoparametric coordinates $(\xi_{A'},\eta_{A'})$ of point A', which are equal to the isoparametric coordinates (ξ_A,η_A). The latter values are then inserted into Eq. (1) as needed to determine the position of point A' in its relaxed state (X_A,Y_A). The relaxed hole surface Γ can thus be determined through the above-described inverse isoparametric mapping as the envelope of all material points that the deformed state reside on the cylindrical drill-bit surface.

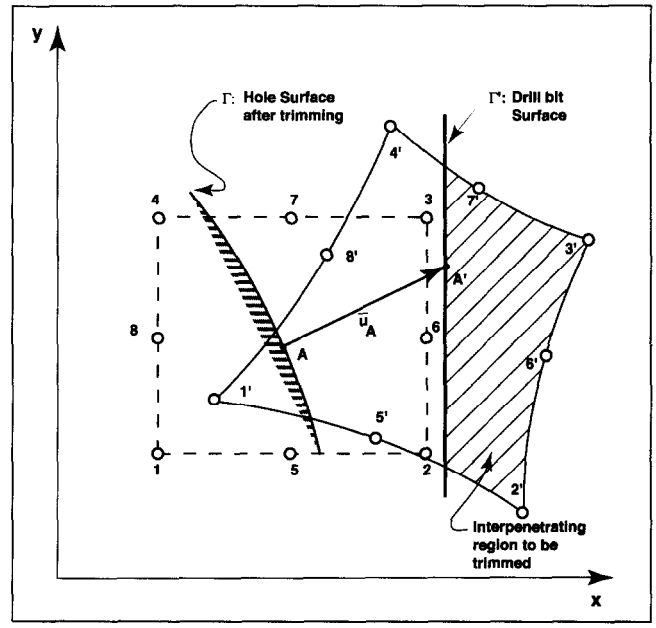

Figure 7
Closeup of Drilled Surface Zone. An eight-noded isoparametric element captures the drill bit surface Γ' in the deformed state. Once the drilling loads are removed, Γ' transforms into surface Γ, which is the shape of the obtained drilled surface.

The above two-dimensional inverse mapping technique was expanded to account for the three-dimensional characteristics of the problem under consideration. The ensuing nonlinear inverse mapping equations are solved with the aid of the Newton's method embedded in a globally convergent strategy.[20]

4. Optimum Design Problem Formulation

A finite element mesh that characterizes the workpiece deformations and details the region around the hole enables one to formulate optimal fixturing as a constrained optimization problem. Here, the objective function Δ is expressed as a function of the design variables $\bar{u}$, as discussed in Section 2. The five selected objective functions denoted as $\Delta_i(\bar{u})$, $i = 1$–5, are discussed in the next section, and their minimum has to reside in the domain defined by the following equilibrium and geometric constraints.

Constraint Formulation

The workpiece has to satisfy static equilibrium constraints:

$$\sum_{j=1}^{n_L} F_{L_j} + \sum_{j=1}^{n_c} F_{c_j} + \sum_{j=1}^{n_F} F_{m_j} + F_w = 0$$
$$\sum_{j=1}^{n_L} T_{L_j} + \sum_{j=1}^{n_c} T_{c_j} + \sum_{j=1}^{n_T} T_{m_j} + T_w = 0 \tag{4}$$

where F_{L_j}, F_{c_j}, F_{m_j}, and F_w are vectorial representations of the locator reaction forces, clamping forces, machining forces, and the weight of the plate, respectively. Also in Eq. (4), T_{L_j}, T_{c_j}, T_{m_j}, and T_w are vectors that contain the moments caused by the locator reaction forces, clamping forces, machining loads and pure torques, and the weight of the plate, respectively. Finally, in Eq. (4) above, n_L, n_c, n_F, and n_T are the number of locators, clamps, machining forces, and moments, respectively. The locator reaction forces have to further be directed toward the workpiece

$$\hat{n}_{L_j} F_{L_j} \geq 0 \tag{5}$$

where $\hat{n}_{L_j}$ is an outband unit normal vector of the jth locator surface. The workpiece also has to maintain resting equilibrium conditions prior to the application of the clamping forces. Resting equilibrium is obtained by constraining the center of gravity of the workpiece (X_W, Y_W) to be within the triangle formed by locators L_1, L_2, and L_3, which must maintain noncollinearity. Resting equilibrium can be expressed mathematically using isoparametric representation of a triangular element

$$0 \leq \xi \leq 1$$
$$\eta \leq 1 - \xi \tag{6}$$

where ξ and η are derived as functions of the coordinates of the center of gravity of the workpiece and the three vertical locators as follows:

$$\xi = \frac{X_w(Y_{L_2} - Y_{L_3}) - Y_w(X_{L_2} - X_{L_3}) + X_{L_2}Y_{L_3} - X_{L_3}Y_{L_2}}{X_{L_1}(Y_{L_2} - Y_{L_3}) + X_{L_2}(Y_{L_3} - Y_{L_1}) + X_{L_3}(Y_{L_1} - Y_{L_2})}$$
$$\eta = \frac{X_w(Y_{L_3} - Y_{L_1}) - Y_w(X_{L_3} - X_{L_1}) + X_{L_1}Y_{L_3} - X_{L_3}Y_{L_1}}{X_{L_1}(Y_{L_2} - Y_{L_3}) + X_{L_2}(Y_{L_3} - Y_{L_1}) + X_{L_3}(Y_{L_1} - Y_{L_2})} \tag{7}$$

The noncollinearity condition can be expressed in terms of the constraining locator coordinates as:

$$X_{L_1}(Y_{L_2} - Y_{L_3}) + X_{L_2}(Y_{L_3} - Y_{L_1}) + X_{L_3}(Y_{L_1} - Y_{L_2}) \geq 0 \tag{8}$$

In addition to satisfying the resting equilibrium condition, one has to enforce clamping equilibrium. The latter is obtained by enforcing (X_{C_1}, Y_{C_1}) to be inside the triangle formed by locators L_1, L_2, and L_3. This constraint results in mathematical expressions that are identical to Eqs. (6) and (7) in which (X_w, Y_w) are replaced with (X_{C_1}, Y_{C_1}). Furthermore, the Y coordinate of C_2 is restricted within the two opposite locators L_4 and L_5. The clamp C_3 has to be directly across from L_6. The physical boundaries of the workpiece define the workspace of the various components of the desired fixture.

To prevent the vertical clamp C_1 and locators L_1, L_2, and L_3 from interfering with the drilling process, the following constraints have to be satisfied:

$$\left(X_{C_1} - X_{o_{nom_k}}\right)^2 + \left(Y_{C_1} - Y_{o_{nom_k}}\right)^2 > R_{nom_k}^2$$
$$\left(X_{L_j} - X_{o_{nom_k}}\right)^2 + \left(Y_{L_j} - Y_{o_{nom_k}}\right)^2 > R_{nom_k}^2, \quad j = 1-3, k = 1-l \tag{9}$$

Here, (X_{o_k}, Y_{o_k}) are the coordinates of the nominal center of the kth hole and R_{nom_k} is its nominal radius. The

clamping forces are constrained to be positive and bounded to prevent undesired plastic deformations:

$$\begin{aligned} 0 \le F_{C_{Z_1}} &\le F^u_{C_{Z_1}} \\ 0 \le F_{C_{X_2}} &\le F^u_{C_{X_2}} \\ 0 \le F_{C_{Y_3}} &\le F^u_{C_{Y_3}} \end{aligned} \tag{10}$$

Equations (4)-(10) constitute the domain in which an optimal fixturing solution is sought. The objective functions are presented in the next section.

Objective Function Formulations

Optimal fixturing solutions are obtained by minimizing one of the following objective functions Δ_1, Δ_2, ..., or Δ_5. These functions capture various measurements of geometric deviations of the machined hole surface. Objective functions Δ_1 and Δ_3 minimize the quadratic difference between the nominal and simulated radii and diameters as they are summed over the entire digitized machine surface. In evaluating Δ_1 and Δ_3, n measurements are taken in a plane, while m planes are measured across the workpiece thickness. These measurements are performed for l holes when sequential or simultaneous drilling operations are used. Thus, Δ_1 and Δ_3 are given by:

$$\Delta_1 = \frac{1}{l.m.n.} \sum_{k=1}^{l} \sum_{j=1}^{m} \sum_{i=1}^{n} \left(R_{nom_k} - R_{ijk} \right)^2 \tag{11}$$

$$\Delta_3 = \frac{1}{l.m.n.} \sum_{k=1}^{l} \sum_{j=1}^{m} \sum_{i=1}^{n} \left(D_{nom_k} - D_{ijk} \right)^2 \tag{12}$$

Here, R_{ijk} and D_{ijk} are the radius and diameter of a point (i,j) at the kth hole and R_{nom_k} and D_{nom_k} are the nominal radius and diameter of the kth hole, respectively.

The maximum differences between the nominal and simulated radii and diameters are captured by the Δ_2 and Δ_4 functions, which are given by:

$$\Delta_2 = Max\left(R_{nom_k} - R_{ijk} \right)^2 \quad i = 1-n, j = 1-m, k = 1-l \tag{13}$$

$$\Delta_4 = Max\left(D_{nom_k} - D_{ijk} \right)^2 \quad i = 1-n, j = 1-m, k = 1-l \tag{14}$$

Note that Δ_2 and Δ_4 address geometric differences that are often used when performing a workpiece tolerance inspection. Objective functions Δ_1 and Δ_2 assume that the nominal location of the center of the hole can be identified, whereas Δ_4 relies on the definition of the hole diameter as it is measured in a machine shop environment.

The Δ_5 objective function measures the deviations of the machined surface from a perfect cylindrical shape. These deviations are captured by calculating for the kth drilled surface the quantities denoted as Θ_k, Ψ_k, and Ω_k that are defined as:

$$\Theta_k = \frac{1}{m.n} \sum_{j=1}^{m} \sum_{i=1}^{n} \left(R_{lsq_j} - \sqrt{\left(X_{ij} - X_{o_j} \right)^2 + \left(Y_{ij} - Y_{o_j} \right)^2} \right)^2 \tag{15}$$

$$\Psi_k = \frac{1}{m} \sum_{j=1}^{m} \left[\left(X_{o_j} - \bar{X}_o \right)^2 + \left(Y_{o_j} - \bar{Y}_o \right)^2 \right] \tag{16}$$

$$\Omega_k = \frac{1}{m} \sum_{j=1}^{m} \left(R_{lsq_j} - \bar{R}_{lsq} \right)^2 \tag{17}$$

In Eq. (15), Θ_k measures the least-square fit of m circles through the coordinates (X_{ij},Y_{ij}) of points that reside on the machined surface. Here, a given j cross section contains n points (i = 1–n). The radii and center coordinates of the least-square fitted circles are denoted as R_{lsq_j}, which is centered at (X_{o_j},Y_{o_j}), respectively. The deviations of center coordinates of the m least-square circles are captured by Ψ_k given by Eq. (16). Here, $\left(\bar{X}_o, \bar{Y}_o\right)$ are the mean values of the center coordinates of the m least-square circles. In Eq. (17), Ω_k measures variations of the radii of the m least-square circles. Here, $\bar{R}_{lsq_j}$ is the mean value of the radii of the m least-square circles. Finally, objective function Δ_5 is a linear combination of the three measures Θ_k, Ψ_k, and Ω_k with designated weights of α, β, and γ:

$$\Delta_5 = \sum_{k=1}^{l} \left[\alpha\Theta_k + \beta\Psi_k + \gamma\Omega_k \right] \tag{18}$$

Proper selection of the α, β, and γ weights is a research topic that has been partially addressed in Wardak.[21] In essence, the above factors highlight the importance of the reciprocal term error as measured through Θ_k, Ψ_k, and Ω_k given by Eqs. (15), (16), and (17), respectively. For example, if $\alpha = 1$, $\beta = 0$, and $\gamma = 0$, objective function Δ_5 is used to minimize Θ_k given by Eq. (15), while relaxing any optimization demands on Ψ_k and Ω_k. This would imply that there is more interest in minimizing the surface roundness while tolerating a relatively inaccurate positioning of the hole. As stated above, an extensive parameter study that addresses proper selections of the factors α, β, and γ is reported in Wardak.[21]

5. Conclusions

A mathematical model that captures the shape and dimensions of drilled surfaces is presented. This model is based on FE analysis and techniques that handle material removal strategies, in which the drill bit is assumed to be rigid. This assumption is legitimate for large-diameter drills. This introduces a limiting factor of the presented model. The formulation focuses on fixturing parameters, such as position of locators, position of clamps, and magnitude of clamping forces, that define the fixturing problem domain. In this domain, optimal fixturing parameters may be found by minimizing a user's selected objective function. Five different objective functions, Δ_1, Δ_2, ..., Δ_5, that capture different geometric characteristics of the machined surface are presented. In Part II of this two-part series of manuscripts, the optimization technique of simulated annealing (SA)[22] is used, and the optimal fixturing layouts are evaluated for different drilling conditions.

Acknowledgment

Support for P.G.C. was provided by the National Science Foundation through a Presidential Young Investigator award, grant CMS94-96209. The authors gratefully acknowledge many helpful discussions with Professor A. Belegundu on the use of optimization algorithms.

References

1. F. Nixon, *Managing to Achieve Quality* (Maidenhead: McGraw Hill), 1971.

2. B. Shirinzadeh, "Issues in the Design of Reconfigurable Fixture Modules for Robotic Assembly," *Journal of Mfg. Systems* (v12, n1, 1993), pp1-13.

3. H. Asada and A. By, "Kinematic Analysis of Workpart Fixturing for Flexible Assembly with Automatically Reconfigurable Fixtures," *IEEE Journal of Robotics and Automation* (vRA-1, n2, 1985), pp86-94.

4. Y. Chou, V. Chandru, M. Barash, and V. Chandru, "Kinematic Analysis of Workpart Fixturing

5. J. Liu and D. Strong, "Survey of Fixture Design Automation," *Trans. of the CSME* (v117, n4A, 1993), pp585-611.

6. R. Brost and K. Goldberg, "A Complete Algorithm for Synthesizing Modular Fixtures for Polygonal Parts," *Proc. of IEEE, Robotics and Automation* (1994), pp535-542.

7. W. Zhang, B. Salunk, P.G. Charalambides, and U. Tasch, "Optimal Fixturing of Rigid and Deformable Bodies," *Proc.* of 3rd IEEE Mediterranean Symp. of New Directions in Control and Automation (v1, July 1995), pp208-219.

8. J. Lee and L. Haynes, "Finite Element Analysis of Flexible Fixturing," *Journal of Engg. for Industry* (v109, n2, 1987), pp134-139.

9. R. Menassa and W. DeVries, "Optimization Methods Applied to Selecting Support Positions in Fixture Design," *Journal of Engg. for Industry* (v113, 1993), pp412-418.

10. C. Pong, "Optimum Fixture Layout Design," PhD thesis (University Park, PA: Pennsylvania State Univ., 1994).

11. E. C. De Meter, "Min-Max Load Model for Optimizing Machining Fixture Performance," *Journal of Engg. for Industry* (v117, 1995), pp186-193

12. S.N. Melkote, "Machining Fixture Layout Optimization Using the Genetic Algorithm," *Int'l Journal of Machine Tools and Manufacture* (v40, 2000), pp579-598.

13. J. Liao, S.J. Hu, and D.A. Stephenson, "Fixture Layout Optimization Considering Workpiece-Fixture Contact Interaction:" Simulation Results" *Trans. of NAMRI/SME* (Vol. XXVI, 1998), pp341-346.

14. W. Cai, S.J. Hu, and J.X. Yuan, "Deformable Sheet Metal Fixturing: Principles, Algorithms, and Simulations," *ASME Journal of Mfg. Science and Engg.* (v118, 1996), pp318-324.

15. Q.A. Sayeed and E.C. De Meter, "Mixed Integer Program Model Fixture Layout Optimization," *ASME Journal of Mfg. Science and Engg.* (v121, 1999), pp701-708.

16. Q.A. Sayeed and E.C. De Meter, "Compliance Based MIP Model and Heuristic for Support Layout Optimization," *Int'l Journal of Production Research* (v37, 1999), pp1283-1307.

17. E.C. De Meter, "Fast Support Layout Optimization," *Int'l Journal of Machine Tools and Manufacture* (v38, 1998), pp1221-1239.

18. ABAQUS/STANDARD, *User's Manual,* version 5.6 (1996).

19. *Tool and Manufacturing Engineers Handbook* (Dearborn, MI: Society of Mfg. Engineers, 1983).

20. W. Press, S. Teukolsky, and W. Vetterling, *Numerical Recipes in Fortran 77, The Art of Scientific Computing* (New York: Cambridge Univ. Press, 1996).

21. K.R. Wardak, "Optimal Fixture Design for Drilling Through Elastically Deforming Plates," PhD thesis (Univ. of Maryland Baltimore County, 1999).

22. A. Corana, M. Marchesi, C. Martini, and S. Ridella, "Minimizing Multimodal Functions of Continuous Variables with the Simulated Annealing Algorithm," *ACM* (v13, Sept. 1987), pp262-280.

Authors' Biographies

Dr. Wardak received his BSc degree in mechanical engineering at the University of Maryland, College Park, in 1992. He obtained his MSc degree in 1994 from the University of Maryland, College Park, also in mechanical engineering. He joined the doctoral program in the Mechanical Engineering Dept. of the University of Maryland, Baltimore County (UMBC) in 1995. He completed his PhD degree in 1999, while conducting research in the area of optimal machine fixture design for deformable workpieces. Dr. Wardak joined Systems Engineering Group, Inc., in 1999. The focus of his current work is in the area of flight dynamics, controls, and optimization of ocean wave dynamics. Dr. Wardak is also a part-time faculty member at UMBC.

Professor Tasch received a BSc degree in mechanical engineering at the Technion Haifa, Israel, in 1976. He obtained a MSc degree at the Illinois Institute of Technology in 1978, and a PhD at the Massachusetts Institute of Technology in 1982, both in mechanical engineering. At Stone and Webster Inc., Dr. Tasch developed a computer-based failure detection system for fossil power plants, and while at The Pennsylvania State University he joined the artificial heart research group and developed the controller of the Penn State heart. In 1989, he joined the Dept. of Mechanical Engineering at the University of Maryland Baltimore County (UMBC), heading the Robotics Laboratory. Dr. Tasch's research contributions include grasping mechanics, fixturing design, and farm automation. He has received the College of Engineering Distinguished Teaching and research awards. He has published 45 technical papers, holds four patents, and has presented his work at many national and international meetings.

Professor Charalambides received his BSc degree in civil engineering from Aristotle University of Thessaloniki, Greece, in 1981. He obtained his MSc and PhD degrees in theoretical and applied mechanics at the University of Illinois at Urbana-Champaign in 1983 and 1986, respectively. During his postdoctoral studies in the Dept. of Materials at the University of California at Santa Barbara, he worked on pioneering studies

with several collaborators on the characterization of bimaterial interface fracture. While at Michigan Technological University (1989-1993), Professor Charalambides received the prestigious NSF-sponsored Presidential Young Investigator award. He joined the Dept. of Mechanical Engineering at the University of Maryland Baltimore County in January 1994. In addition to the fracture of bimaterial interfaces and delamination in layered systems, Dr. Charalambides' research contributions include studies on micromechanical modeling, the modeling of unidirectionally reinforced composites, woven ceramic matrix composites, biomechanics, optimal fixturing in manufacturing, and technology transfer through software development. He received the Michigan Tech Distinguished Teacher of the Year Award and the State of Michigan Teaching Excellence Award. He has published over 40 technical papers and has presented his work at numerous national and international forums.